Electronic Supplementary Information for: Capturing CO$_2$ by Ceria and Ceria-zirconia Nanomaterials of Different Origin

D. Panayotov,[1,*] V. Zdravkova,[1] O. Lagunov,[1] S. Andonova,[1] I. Spassova,[1] D. Nihtianova,[2] G. Atanasova,[1] N. Drenchev,[1] E. Ivanova,[1] M. Mihaylov,[1] K. Hadjiivanov[1]

[1]Institute of General and Inorganic Chemistry, Bulgarian Academy of Sciences, "Acad. G. Bonchev" str. bl.11, 1113 Sofia, Bulgaria
[2]Institute of Mineralogy and Crystallography, Bulgarian Academy of Sciences, "Acad. G. Bonchev" str. bl.107, 1113 Sofia, Bulgaria

1. Experimental

1.1. Nanoscale CeO$_2$-based materials

Two commercial CeO$_2$ powder materials having similar nanoscale particle sizes and specific surface areas were obtained from Alfa Aesar (99.5% purity) and US Research Nanomaterials (99.99% purity). These samples were designated as CeO$_2$-AA and CeO$_2$-USRN, respectively, and their characteristics are shown in Table 1. Another pure CeO$_2$ sample, designated as CeO$_2$, was prepared by precipitation with 25% ammonia (Neochim) method[1] using Ce(NO$_3$)$_3$.6H$_2$O (Fluka AG, 99 %) as the Ce^{3+} precursor. The CeO$_2$(75%)-ZrO$_2$(25%) mixed oxide sample, designated CeO$_2$–ZrO$_2$, was prepared by coprecipitation with ammonia using the same Ce^{3+} precursor and ZrO(NO$_3$)$_2$.xH$_2$O (Alfa Aesar, 99.9 %). In these preparations 200 cm^3 of 0.1 M aqueous solution of Ce(NO$_3$)$_3$.6H$_2$O (and respective ZrO(NO$_3$)$_2$.xH$_2$O with the required molar ratio) were added dropwise to 100 cm^3 of NH$_4$OH (25%), while exposed to ultrasonic irradiation that lasted 20 min. The resulting precipitates were filtered and washed with deionized water to pH 9, followed by drying in air at 373 K overnight. The samples were finally heated at a rate of 5 K min^{-1} in a stream of air (200 cm^3 min^{-1}) and calcined for 1 hour at 773 K. The characteristics of home-synthesized CeO$_2$ and CeO$_2$–ZrO$_2$ samples are also shown in Table 1.

1.2. XRD analysis

The powder X-ray diffraction analysis was performed on a Bruker D8 Advance diffractometer with Cu Kα radiation using a Lynx Eye detector. The XRD patterns were collected within the range 20–80° of 2θ with a step size of 0.02° s^{-1}. Mean crystallite sizes were determined with the Topas-4.2 software package using the fundamental parameters peak shape description, including appropriate corrections for the instrumental broadening and diffractometer geometry.

1.3. TEM analysis

The Transmission Electron Microscopy (TEM)/High-Resolution Transmission Electron Microscopy (HRTEM) patterns were taken with a JEOL 2100 transmission electron microscope at accelerating voltage of 200 kV equipped with X-ray energy-dispersive spectrometer (XEDS) Oxford Instruments, X-MAX N 80 T; CCD Camera ORIUS 1000, 11 Mp, GATAN. Before examination, each oxide sample was suspended in ethanol solution and dripped onto standard holey carbon/Cu grid. The nanoparticle size distribution was determined by image processing software Image J. The measurements of lattice-fringe spacing recorded in HRTEM micrographs were made using digital image analysis of reciprocal space parameters. The analysis of data was carried out by the Digital Micrograph software.

1.4. Raman spectra

Raman spectra were recorded on Raman Microscope Senterra II (Bruker) instrument. The powder samples (approximately 10 mg) were mechanically dispersed onto a glass plate and analyzed using the vertical 20x objective in an 180° backscattering arrangement. The Raman spectrometer parameters used include: 6.5 mW laser power at 532 nm wavelength and an exposure time of 100 seconds; the resolution was 1 cm^{-1} for all the spectra.

1.5. XPS analysis

The XPS measurements were carried out on AXIS Supra electron spectrometer (Kratos Analitycal Ltd.) using Al Kα radiation with photon energy of 1486.6 eV. The energy calibration was performed by normalizing the C1s line of adsorbed adventitious hydrocarbons to 284.6 eV. The binding energies (BE) were determined with accuracy of ±0.1 eV using the commercial data-processing software ESCApeTM of Kratos Analytical Ltd. The concentration of the different chemical elements (in atomic %) was calculated by normalizing the area of the photoelectron peaks to their relative sensitivity factors. The deconvolution of the peaks has been performed by using the commercial data-processing software ESCApeTM of Kratos Analytical Ltd. Before the X-rays irradiation the samples were stored overnight in the ultra-high vacuum (UHV) chamber. Note that due to a known (and observed) impact of X-rays irradiation on CeO_2 nanoparticles (under UHV-conditions) that can transform Ce^{4+} to Ce^{3+},[2-4] only the data from the first measurement for each specimen are reported here. The surface concentration of Ce^{3+} cations given in Fig. 2(b), panel A was calculated from the intensity of the v_o (u_o) and v' (u') lines, according to the equation given in previous works:[1, 5]

$$Ce^{3+}(\%) = \frac{v_0 + v^{'} + u_0 + u^{'}}{\sum (v + u)} \quad (1)$$

1.6. H_2–TPR experiments and CO_2-TPD experiments

The H_2–TPR and CO_2–TPD experiments were performed using ChemBET TPR/TPD (Quantachrome Instruments) apparatus equipped with thermal conductivity detector (TCD). An

ethanol trap cooled down to 210 K was used to eliminate water vapor from the gas flow. The H_2–TPR experiments were carried out with samples (80 mg, 0.25–0.4 mm granules) heat-treated in 20 cm^3 min^{-1} of He flow from 293 to 773 K (at a rate of 20 K min^{-1}) and then oxidized at 773 K for 30 min in a flow of 5 vol.% O_2 in He flow (20 cm^3 min^{-1}). After that, the samples were cooled down to 423 K in the same flow and from 423 K to 293 K in a flow of He. The H_2–TPR experiments were performed in 10 vol.% H_2 in Ar flow (20 cm^3 min^{-1}) from 293 K to 1273 K at a heating rate of 10 K min^{-1}.

The CO_2–TPD experiments were carried out with samples (80 mg, 0.25–0.4 mm granules) that were either oxidized or reduced. The oxidation of samples was performed as follows: the samples were heat-treated in 20 cm^3 min^{-1} of He flow from 293 to 773 K (at a rate of 20 K min^{-1}) and then oxidized at 773 K for 30 min in a flow of 5 vol.% O_2 in He flow (20 cm^3 min^{-1}). After that, the samples were cooled down to 423 K in the same flow and from 423 K to 323 K in a flow of He. The reduction of samples was carried out in 10 vol.% H_2 in Ar flow (20 cm^3 min^{-1}) from 293 K to the desire temperature (648 K or 723 K) at a heating rate of 10 K min^{-1}. The samples were then cooled down to 373 K in the same flow and from 373 K to 323 K in a He flow. The adsorption of CO_2 was done under exposure to a flow of 600 ppm CO_2 in Ar (20 cm^3 min^{-1}) for 30 min at 323 K, then subjected to a He flow (20 cm^3 min^{-1}) and kept under these conditions for 30 min. The CO_2–TPD measurements were performed in a He flow (20 cm^3 min^{-1}) from 323 to 683 K at a heating rate of 10 K min^{-1}. Because of the use of a nonselective TC detection, the measured CO_2–TPD profiles may contain some contribution from other desorbing gases/vapors.

Gases and gas mixtures (all supplied from Messer) used in the H_2–TPR and CO_2–TPD experiments: He (99.999 %), 5 vol.% O_2/He (O_2 99.95 %), 10 vol.% H_2/Ar (H_2 99.95 %) and 0.06 vol.% CO_2/Ar (CO_2 99.95 %).

1.7. N_2- and CO_2-adsorption isotherms

The texture characteristics of the samples were determined by low-temperature (77.4 K) nitrogen physisorption in a static volumetric Quantachrome NOVA 1200e instrument (USA). The adsorption-desorption isotherms were analyzed to obtain the specific surface area, total pore volume and average pore diameter. The specific surface areas (S_{BET}) were calculated on the basis of the Brunauer-Emmett-Teller equation, the total pore volumes and average pore diameters (V_t) were estimated at a relative pressure ~0.99 according to the Gurvich rule. The pore-size distribution (PSD) was calculated by Barrett-Joyner-Halenda (BJH) method. The static CO_2 adsorption experiments were performed at 273 K in the same instrument. Prior to each adsorption measurement, the sample was degassed under dynamic vacuum of $< 1×10^{-2}$ Pa at 423 K for 18 h.

Pure gases N_2 (99.999 %) and CO_2 (99.998 %) were supplied from Messer.

1.8. Dynamic CO_2 adsorption (breakthrough) experiments

The breakthrough experiments for CO_2 adsorption under dynamic conditions were carried out on a CATLAB system Hiden Analytical (Warrington, UK) equipped with an HPR-20 R&D quadrupole mass spectrometer (MS). The system allowed a stream of Ar carrier gas or Ar + CO_2 gas mixture to be passed at a flow rate of 20 cm^3 min^{-1} through a column containing the tested adsorbent sample (100 mg, 0.25–0.4 mm granules) as a fixed bed (column diameter D = 7 mm, total bed height H_T = 5 mm) that was conditioned at ~323 K. The concentration of CO_2 in the Ar + CO_2 gas stream was typically 300 ppm CO_2 and the gas flow rate 20 cm^3 min^{-1}. In some experiments, concentration of 200 ppm CO_2 and gas flow rate of 50 cm^3 min^{-1} were applied and this is especially noted in the text. The inlet gas composition was controlled by a system of individual mass flow controllers (Bronkhorst Hi–Tech). The effluent gas composition was monitored by the MS using a heated capillary probe that was directly connected to the exit of the reactor. The breakthrough (the first evidence of CO_2 in the effluent gas) and the CO_2-TPD analysis were performed by recording the MS signals with mass to charge ratio (m/e) equal to 44 in pressure units *vs.* time mode. The MS signals with m/e = 18 (H_2O) and m/e = 28 (N_2) were also followed. Prior to each measurement, the adsorbent sample was first degassed in a flow of Ar (20 cm^3 min^{-1}) at 773 K for 1 h. The sample was further activated in 1 vol.% O_2/Ar flow (20 cm^3 min^{-1}) at 773 K for 1h. After that, the temperature was decreased to 323 K and the sample was flushed with the Ar flow. Following the activation the sample was exposed to the Ar + CO_2 flow and the breakthrough curve was recorded. When the sample saturation with CO_2 was achieved the gas mixture was switched back to the Ar flow for 90 min. Afterwards, the CO_2 temperature programmed desorption (CO_2-TPD) was carried out under the Ar flow (20 cm^3 min^{-1}) at a heating rate of 10 K min^{-1} from 323 to 773 K. The CO_2-TPD data allow determining the optimum temperature for the adsorbent regeneration. The total CO_2 captured amount (μmol g^{-1}) during the dynamic adsorption experiment was calculated using Eq. (1):

$$[CO_{2,ads}] = (CO_{2,in})t_A - (CO_{2,out})t_A \qquad\qquad\qquad \text{Eq. (1)}$$

$(CO_{2,in})t_A$ is the total integrated CO_2 concentration at the reactor inlet during the adsorption period (C_0, μmol g^{-1}), $(CO_{2,out})t_A$ is the total integrated CO_2 concentration at the reactor outlet during the adsorption period (C, μmol g^{-1}) and t_A is the length of the adsorption period (min) until the saturation point is achieved, i.e. the point where the $(CO_{2,out})$ and $(CO_{2,in})$ equilibrate. Some of the experimental kinetic breakthrough data were further processed using the nonlinear curve fitting procedure from the Origin 2017 software (OriginLab Corp). The experimental setup included a water vapor leaking system allowing to perform measurements of the CO_2 dynamic adsorption in the presence of trace amounts of water vapors. The partial pressure of H_2O in the gas flow of CO_2+Ar, as measured by the MS signal with m/e = 18 was one order of magnitude higher than that measured under dry (without H_2O traces) conditions (~ 1×10^{-11} kPa).

Gases and gas mixtures (all supplied from Messer) used in the breakthrough experiments: Ar (99.999 %), 0.06 vol.% CO_2/Ar (CO_2 99.95 %), 5 vol.% O_2/Ar (O_2 99.95 %), 0.06 vol.% H_2/Ar (H_2 99.95 %).

1.9. FTIR spectroscopy measurements

FTIR spectra were registered with a FTIR Spectrometer Thermo Scientific Nicolet iS 5 at a spectral resolution of 2 cm^{-1} and accumulating up to 256 scans. Self-supporting wafers (ca. 10 mg cm^{-2}) were prepared from the powder samples and treated directly in a purpose-made IR cell. The latter was connected to a vacuum-adsorption apparatus with a residual pressure below 1×10^{-4} Pa. Prior to each CO_2 adsorption experiment, the samples were subjected to two different pre-treatment procedures: i.e. activation in O_2 or reduction in H_2. The O_2-activation procedure included evacuation of sample from 293 to 773 K under dynamic vacuum $< 1\times10^{-4}$ Pa, keeping at 773 K for 60 min, first oxidation step in 2 kPa O_2 at 773 K for 30 min, evacuation at 773 K for 2 min and a second oxidation step under the same condition. After that the sample was cooled down to 298 K and evacuated. The H_2-reduction procedure included evacuation of the sample at 773 K and $< 1\times10^{-4}$ Pa pressure for 60 min, a first reduction step in 2 kPa H_2 at 773 K for 30 min, evacuation at 773 K for 2 min and a second reduction step under the same conditions. After that, the sample was evacuated and cooled down to 298 K under dynamic vacuum. The adsorption of CO_2 was performed upon exposing the sample to 2 kPa CO_2 at 298 K for 30 min and subsequent evacuation at 298 K for 60 min. The sample was then heat-treated in dynamic vacuum under stepwise elevation of temperature between 323 and 673 K at a step of 50 K. The samples were kept for 10 min at each selected temperature within this range. The adsorption of H_2O was made by exposure of activated samples to consecutive small doses (0.2 kPa) of H_2O vapor until saturation in the ν(OH) region of the IR spectrum is achieved. The samples were then evacuated at 298 K for 60 min. In one set of experiments, the water pre-covered sample was subjected to heat-treatment in dynamic vacuum at elevated temperatures in the range 323 - 673 K as already described above. In other set of experiments, a water pre-covered sample was exposed to CO_2 following the same procedure as that applied to water-free samples described above.

Carbon dioxide (99,9993 %) was supplied from Linde Gaz Magyarorszag ZRt. Both oxygen (99.999%) and hydrogen (99.999%) were purchased from Messer. The gases O_2 and H_2 were additionally purified by passing through a liquid nitrogen trap.
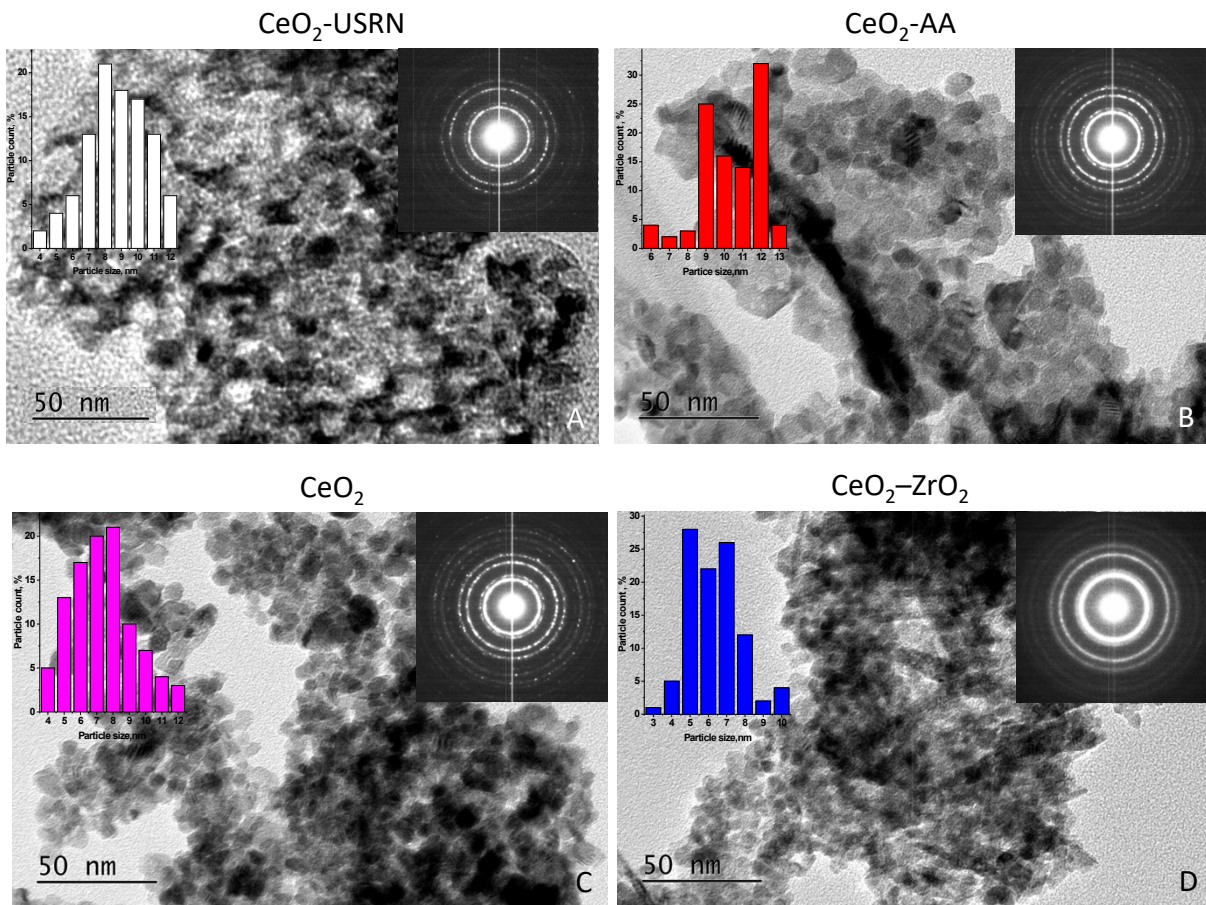
2. Figures

Figure S1. TEM bright field micrographs of the four studied samples. Particle size distributions (left insets) and selected area electron diffractions (right insets).
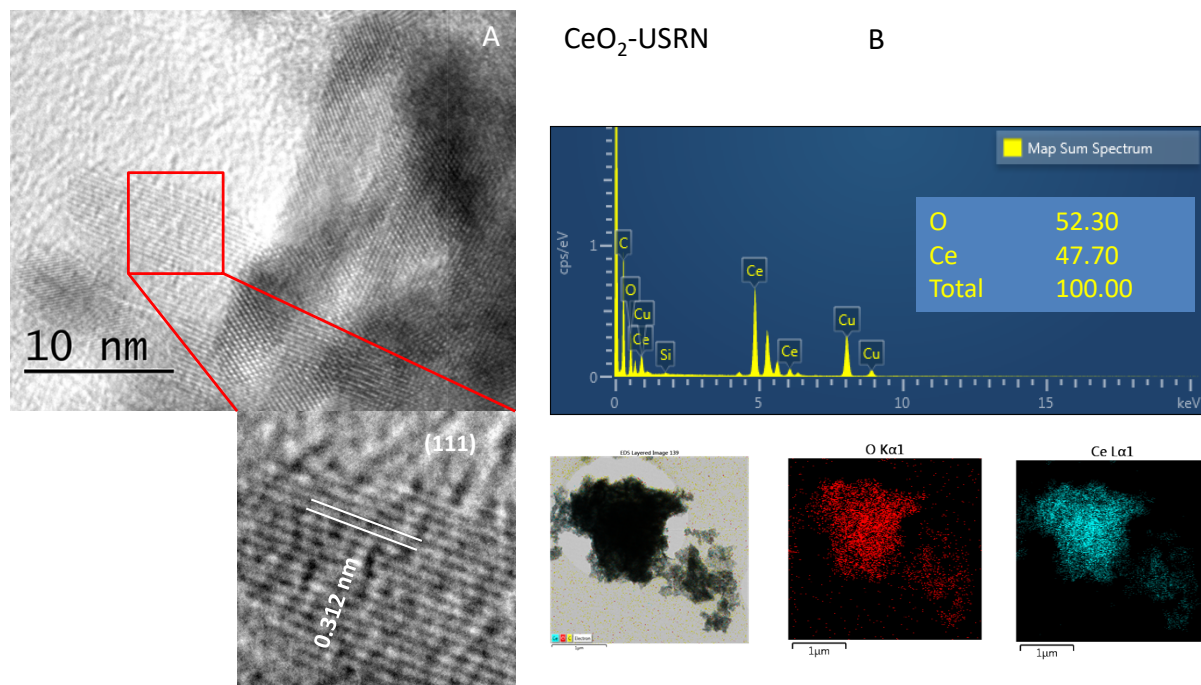
Figure S2. Experimental HRTEM image and a Fourier filtered one-dimensional HRTEM image of CeO$_2$-USRN sample (A). XEDS elemental mapping and corresponding spectrum (B).
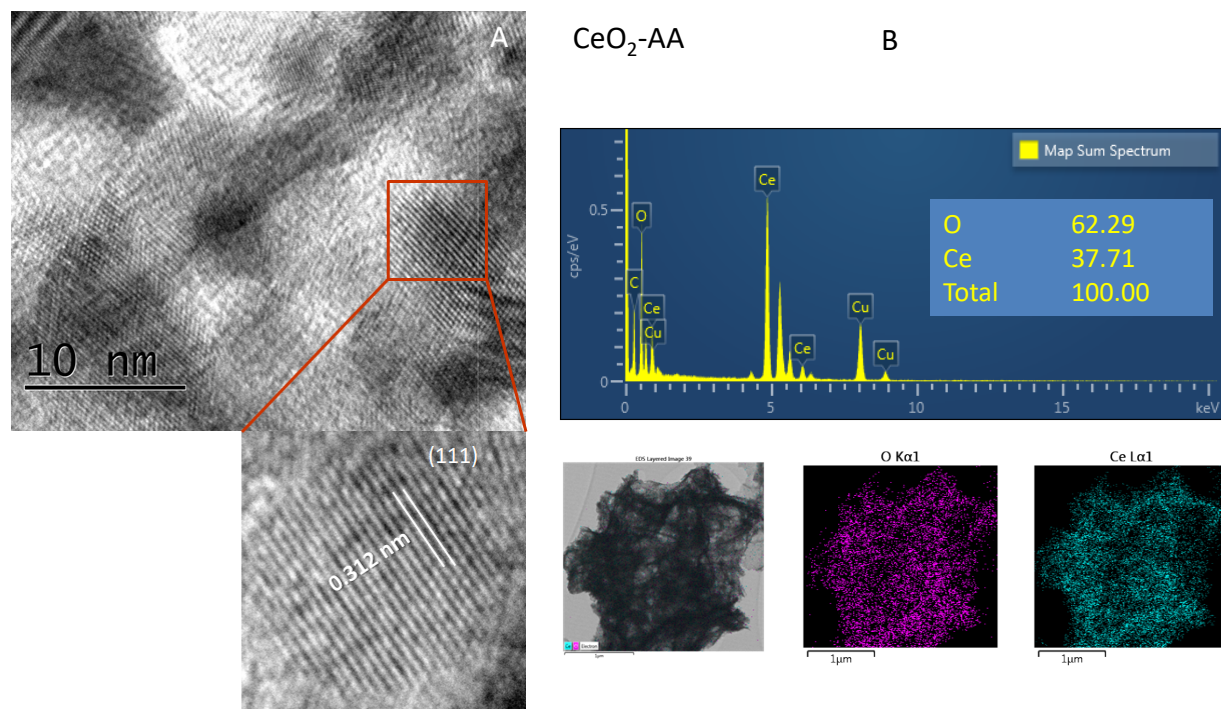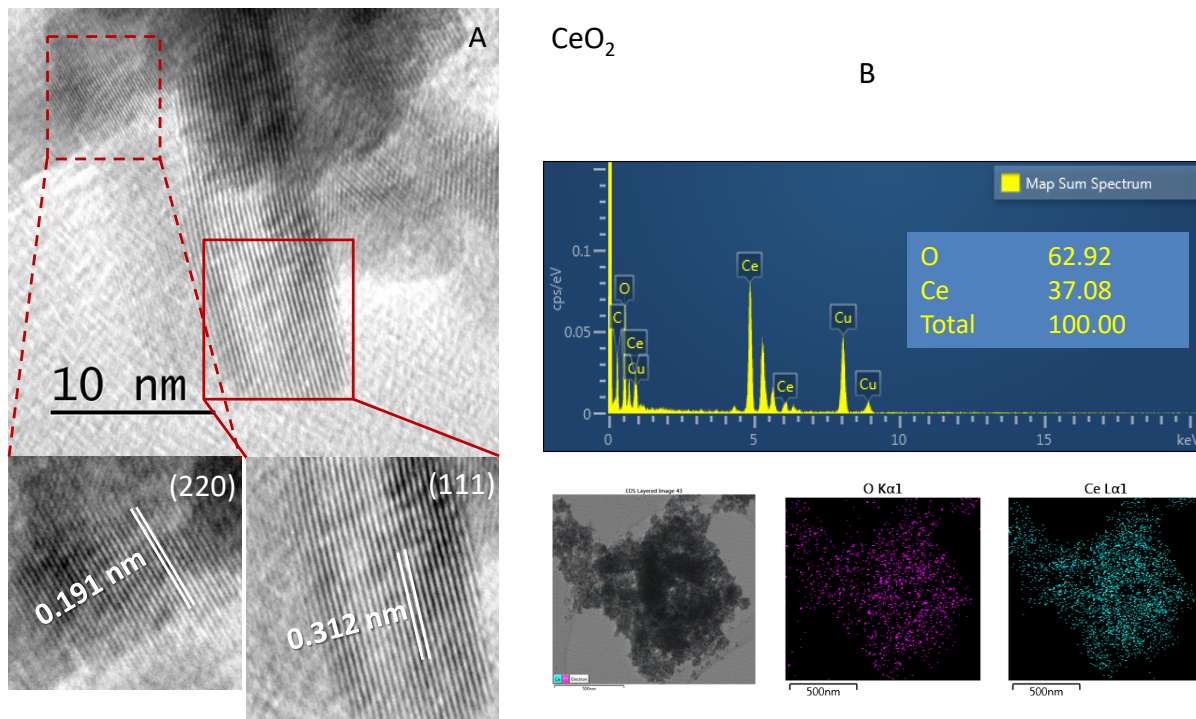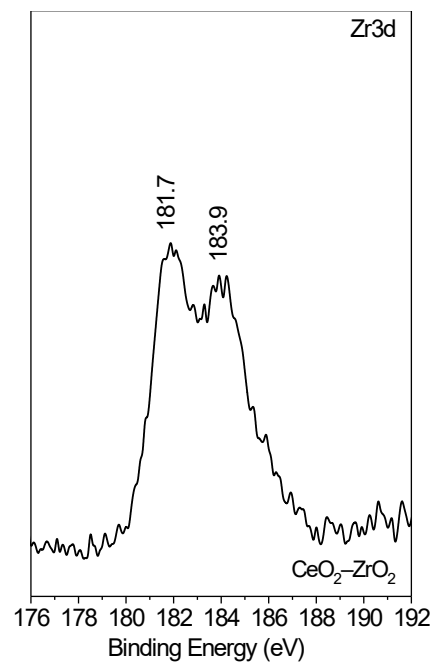
Figure S3. Experimental HRTEM image and a Fourier filtered one-dimensional HRTEM image of CeO$_2$-AA sample (A). XEDS elemental mapping and corresponding spectrum (B).

Figure S4. Experimental HRTEM image and Fourier filtered one-dimensional HRTEM images of CeO_2 sample (A). XEDS elemental mapping and corresponding spectrum (B).

Figure S5. Zr $3d_{5/2}$ XPS spectrum of the CeO_2–ZrO_2 sample.
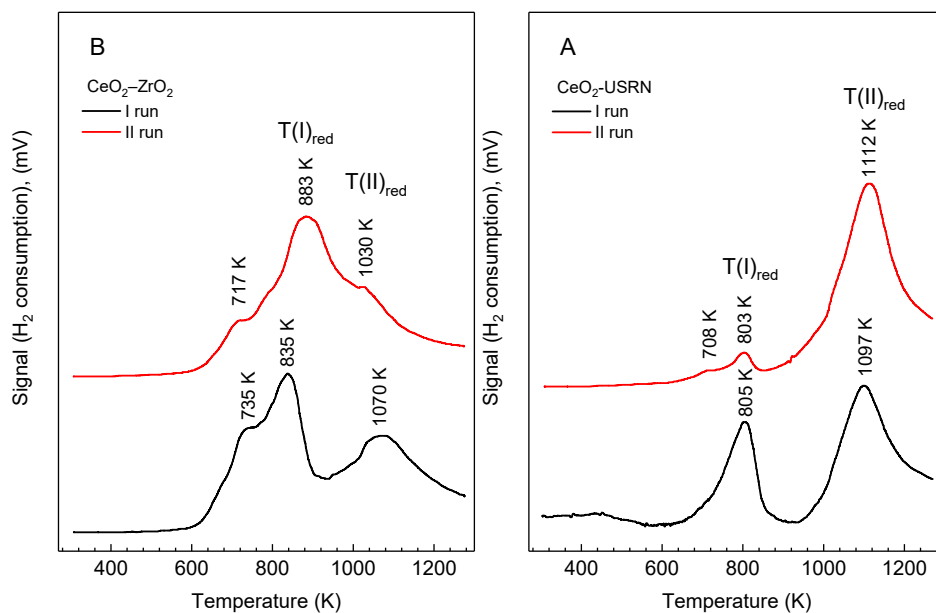
Figure S6. (A, B) H$_2$-TPR profiles obtained in two consecutive experiments with O$_2$-activated (773 K) samples carried out with 10 vol.% H$_2$/Ar flow (20 cm^3 min^{-1}) from 293 K to 1273 K at a heating rate of 10 K min^{-1}.
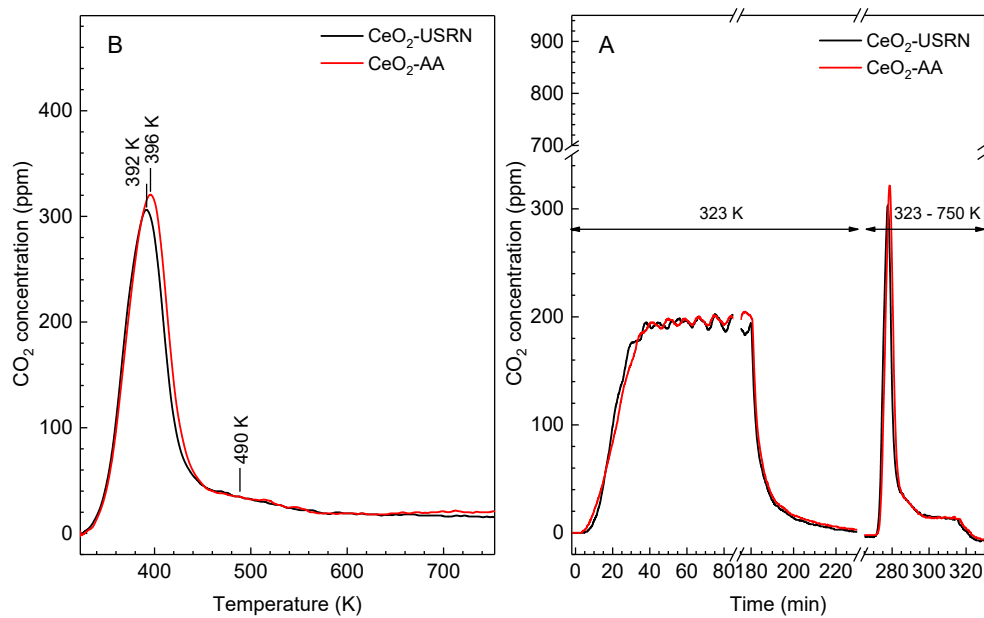
Figure S7. (A) Dynamic CO_2 saturation (breakthrough) curves obtained with O_2-activated (773 K) samples in a flow of 200 ppm CO_2+Ar (50 cm^3 min^{-1}) at 323 K and TD curves obtained in an Ar flow; (B) TPD profiles of the CO_2 evolution as obtained in the dynamic experiments (C).

B

CeO$_2$-USRN
CeO$_2$
CeO$_2$–ZrO$_2$

d[(CO$_{2,out}$)/(CO$_{2,in}$)]/dt,

II III
I IV

Time (min)

A

(CO$_{2out}$)/(CO$_{2,in}$)

Model	Slogistic1
Equation	y = a/(1 + exp(-k*(x-xc)))
Plot	C
a	0.96877
xc	34.00147
k	0.19532
Reduced Chi-Sqr	1.60371E-4
R-Square(COD)	0.99905
Adj. R-Square	0.99905

Model	Slogistic1
Equation	y = a/(1 + exp(-k*(x-xc)))
Plot	C
a	1.00005
xc	48.00147
k	0.05274
Reduced Chi-Sqr	3.41203E-4
R-Square(COD)	0.99665
Adj. R-Square	0.99663

Model	Slogistic1
Equation	y = a/(1 + exp(-k*(x-xc)))
Plot	C
a	0.96877
xc	56.00147
k	0.11328
Reduced Chi-Sqr	6.8409E-4
R-Square(COD)	0.9958
Adj. R-Square	0.99578

CeO$_2$-USRN
CeO$_2$
CeO$_2$–ZrO$_2$

Time (min)

Figure S8. (A) Dynamic CO$_2$ saturation (breakthrough) curves recalculated as $(CO_{2,out})/(CO_{2,in})$ *vs* time graphs from Figure 4C. (B) Rate profiles d[$(CO_{2,out})/(CO_{2,in})$]/dt *vs* time.
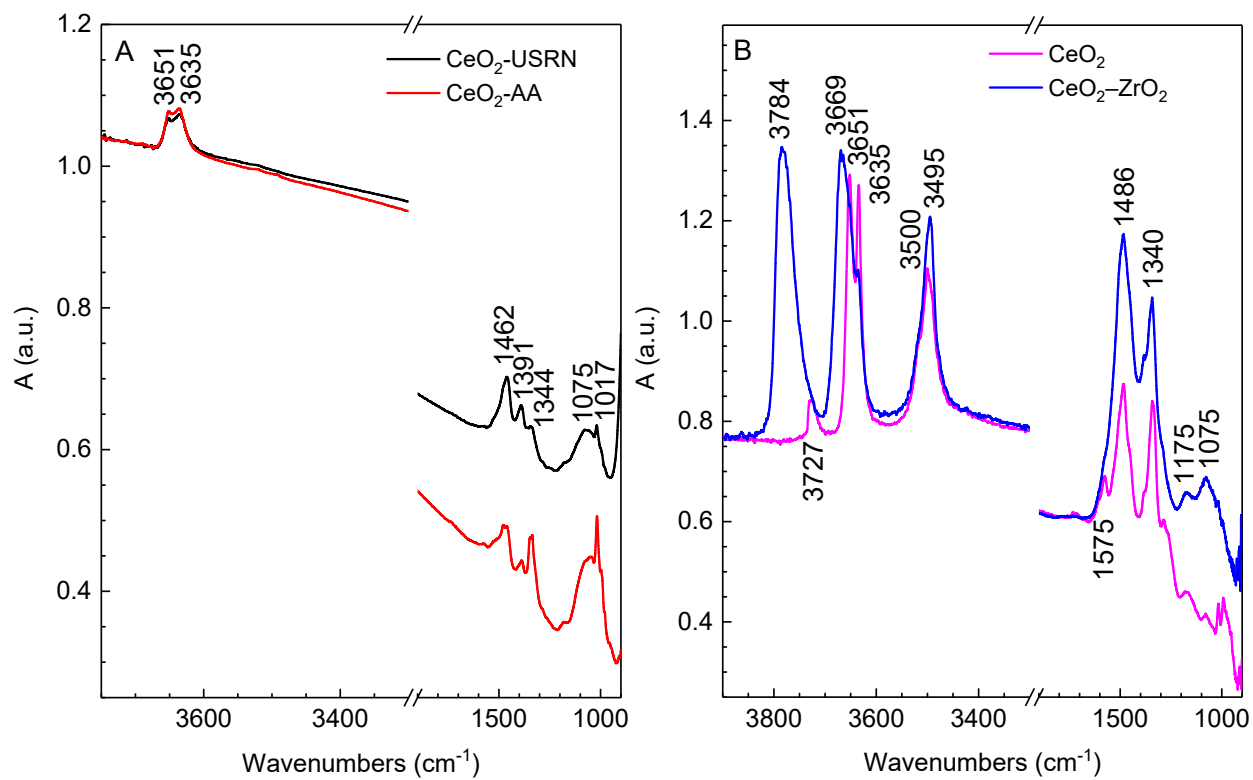
Figure S9. FTIR spectra of the O_2-activated at 773 K samples: (A) CeO_2-USRN and CeO_2-AA; (B) CeO_2 and CeO_2–ZrO_2. The spectra are acquired under vacuum 1×10^{-4} Pa at 293 K.
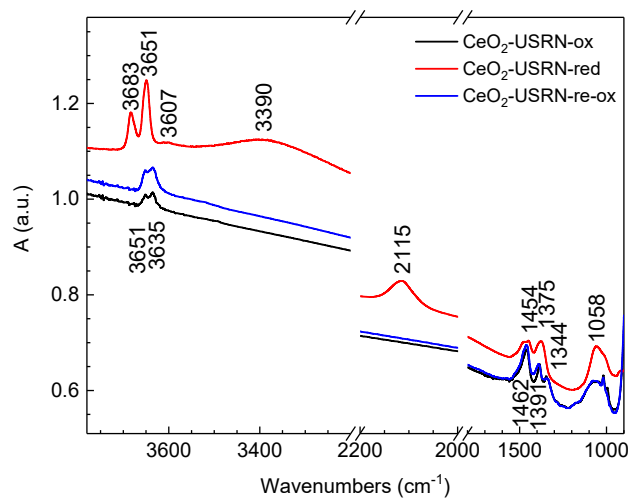
Figure S10. FTIR spectra of the CeO$_2$-USRN sample: O$_2$-activated at 773 K, H$_2$-reduced at 773 K and O$_2$-reactivated at 773 K, spectra acquired under vacuum 1×10^{-4} Pa at 293 K.
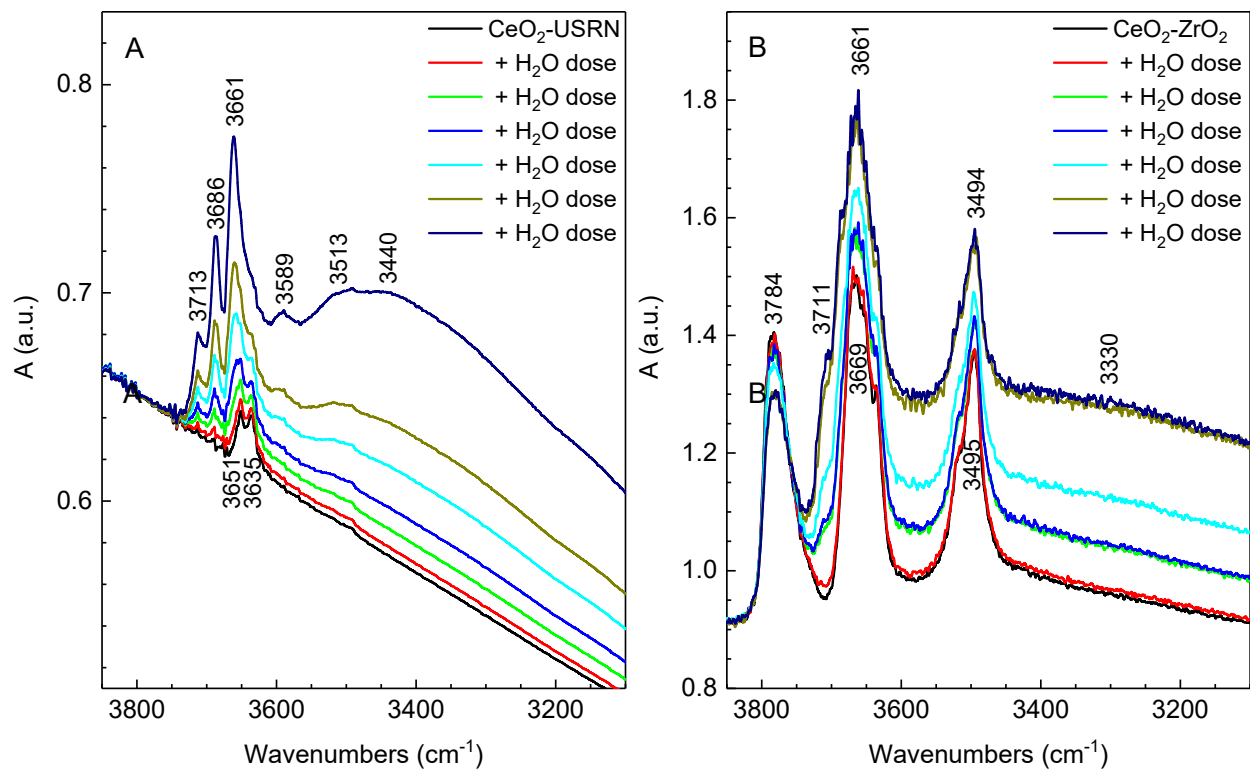
Figure S11. FTIR spectra of: (A) CeO2-USRN and (B) CeO2-ZrO2, after adsorption of multiple doses of H_2O at 293 K on O_2-activated samples.
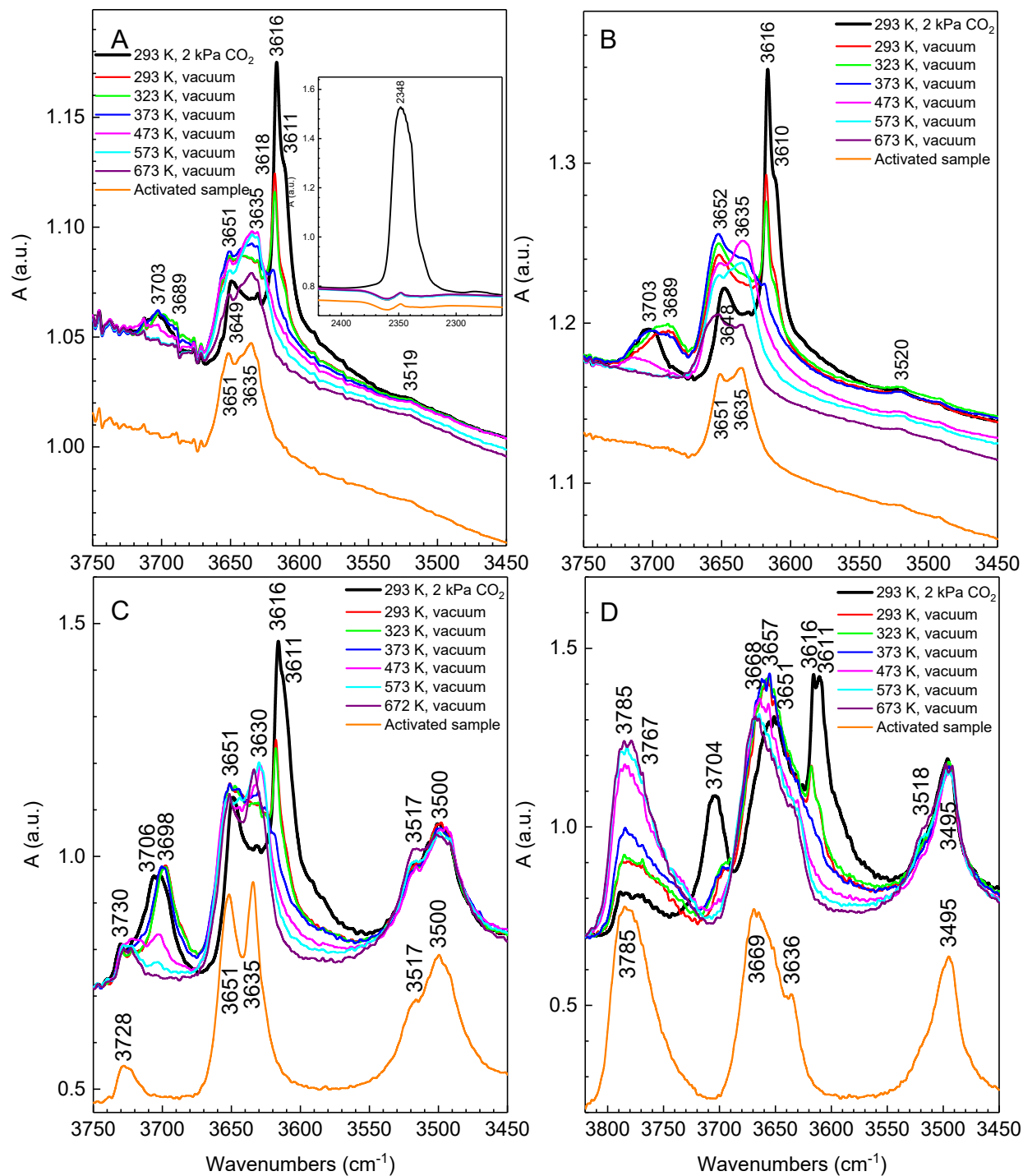
Figure S12. FTIR spectra in the OH-region of O_2-activated samples obtained after adsorption of 2 kPa (equilibrium pressure) CO_2 at 293 K (black) and evacuation for 10 min at 293 K and elevated temperatures: (A) CeO_2-USRN; (B) CeO_2-AA; (C) CeO_2; (D) CeO_2–ZrO_2. See the corresponding spectra in Fig. 7.
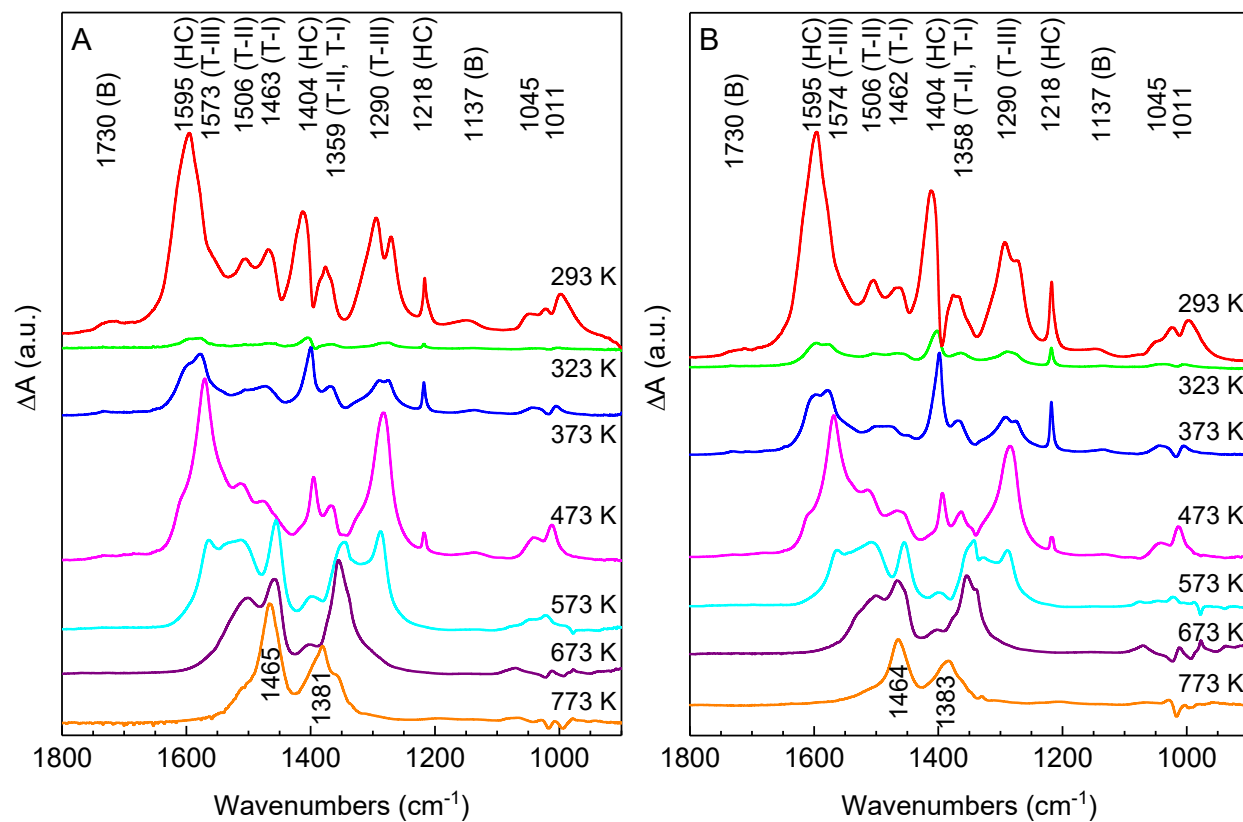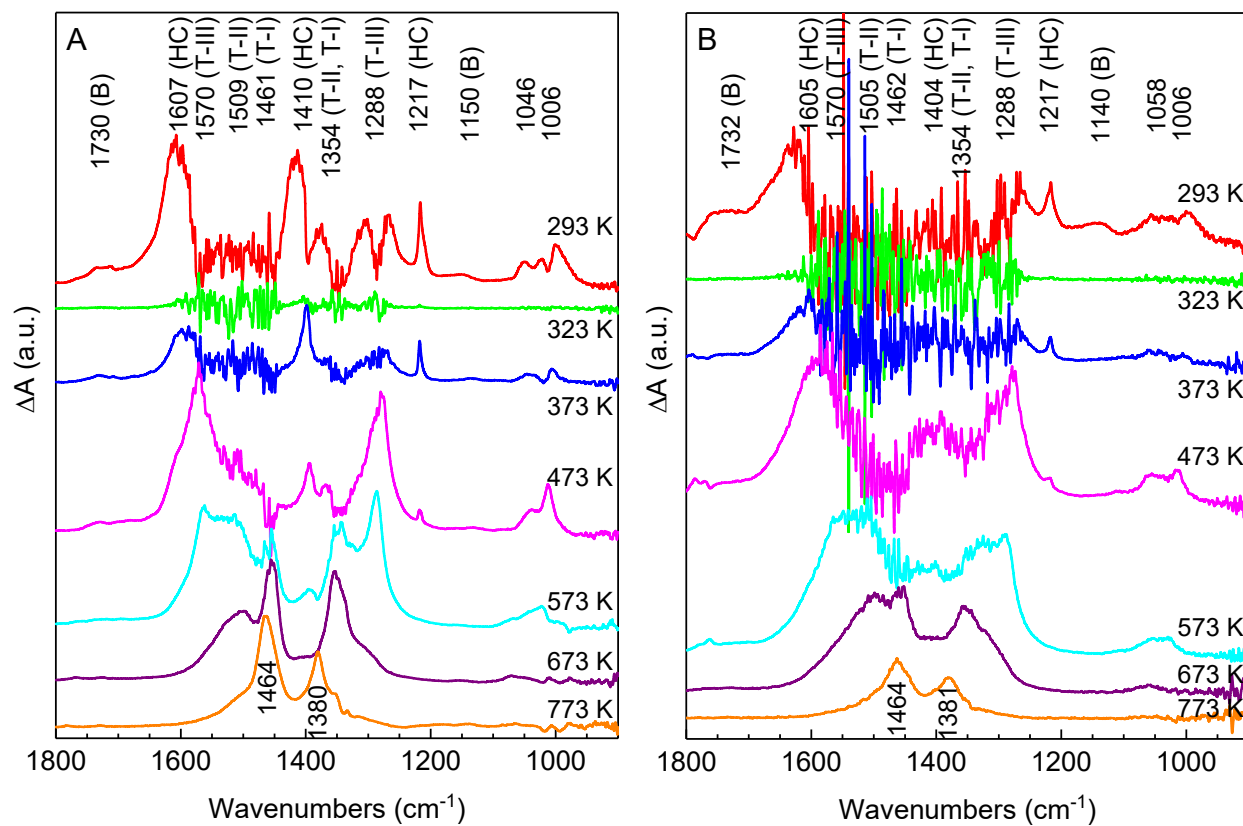
Figure S13. Difference FTIR spectra obtained during the stepwise thermal desorption of CO_2 preadsorbed on activated samples: (A) CeO_2-USRN and (B) CeO_2-AA. See the corresponding spectra in Figs. 7A and 7B, respectively.
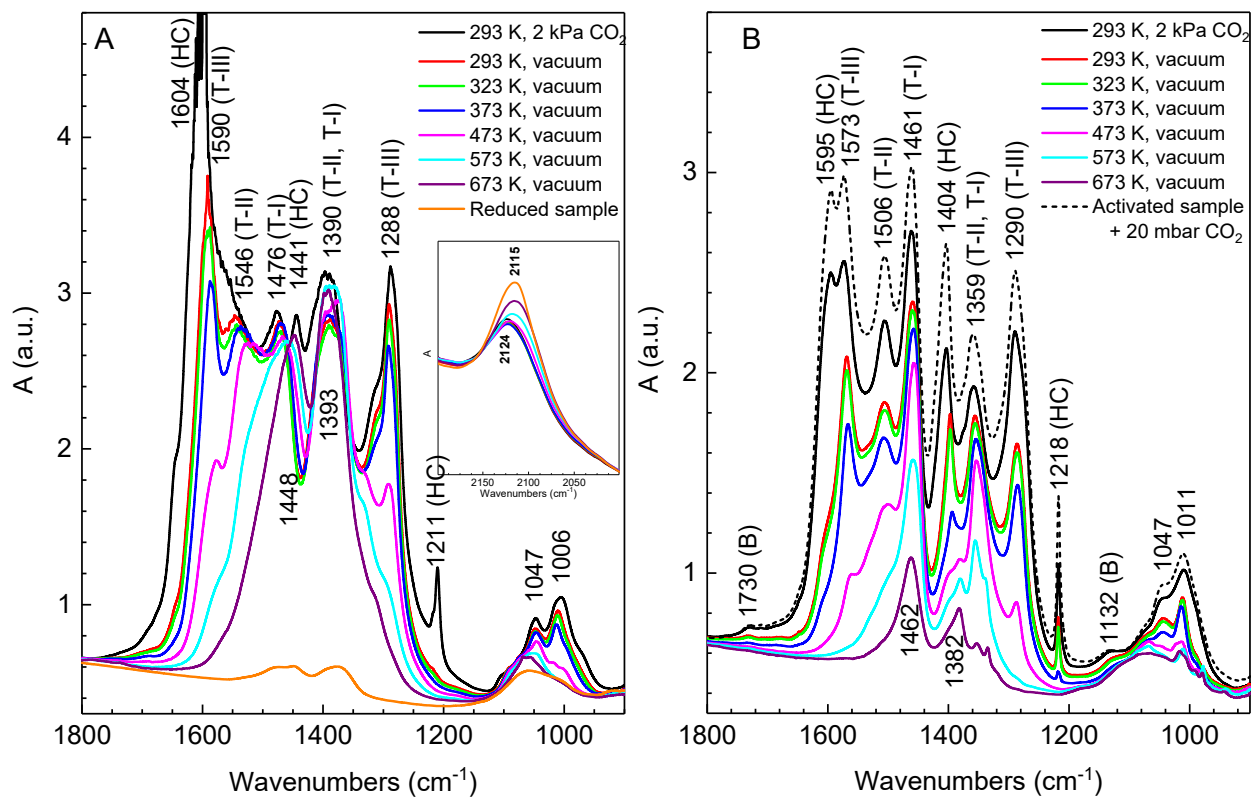
Figure S14. Difference FTIR spectra obtained during the stepwise thermal desorption of CO_2 preadsorbed on activated samples: (A) CeO_2 and (B) CeO_2–ZrO_2. See the corresponding spectra in Figs. 7C and 7D, respectively.

Figure S15. FTIR spectra of H_2-reduced (A) and then O_2-reactivated CeO_2-AA (B) sample obtained after adsorption of 2 kPa (equilibrium pressure) CO_2 at 293 K (black) and after evacuation for 10 min at 293 K and elevated temperatures (red to purple, as noted). The dash-lined spectrum in (B) is that obtained with the activated sample, Fig. 7B.
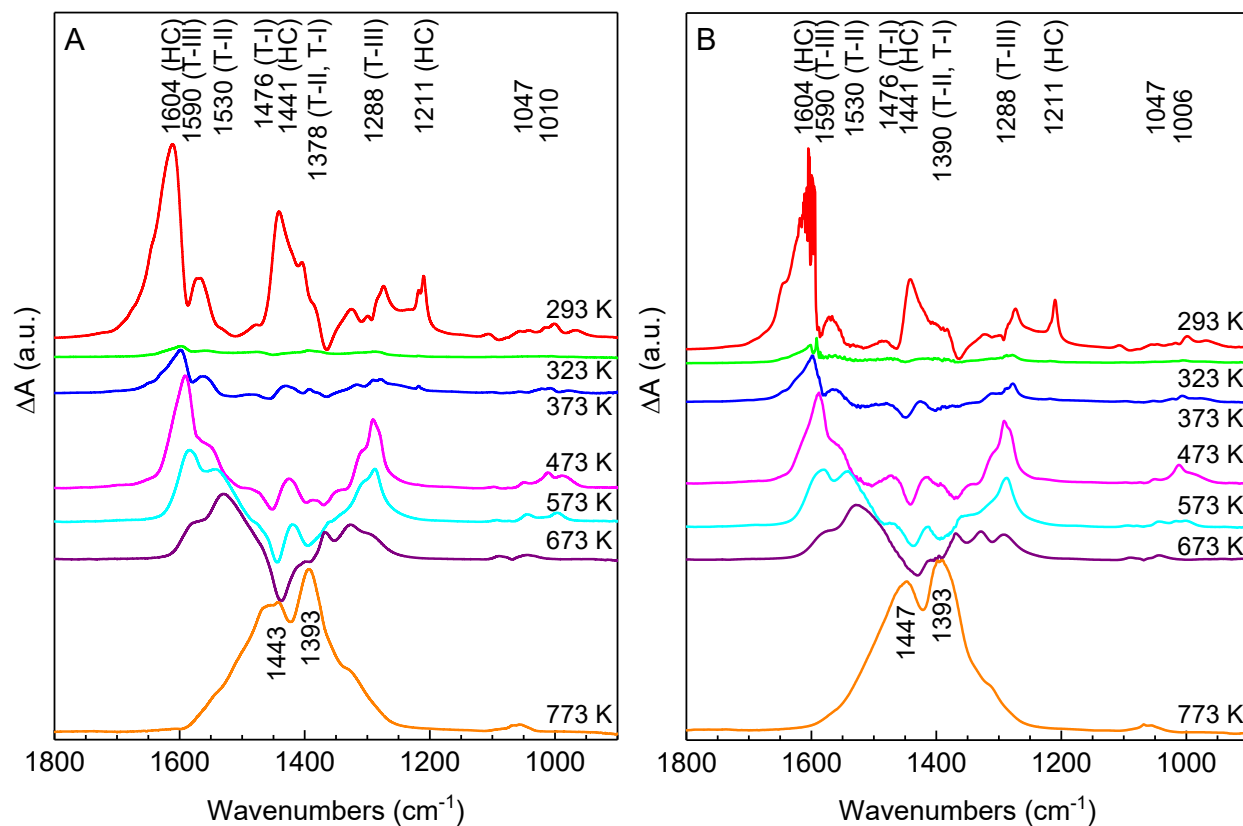
Figure S16. Difference FTIR spectra obtained during the stepwise thermal desorption of CO_2 preadsorbed on reduced samples: (A) CeO_2-USRN and (B) CeO_2-AA. See the corresponding spectra in Figs. 8A and S15A, respectively.
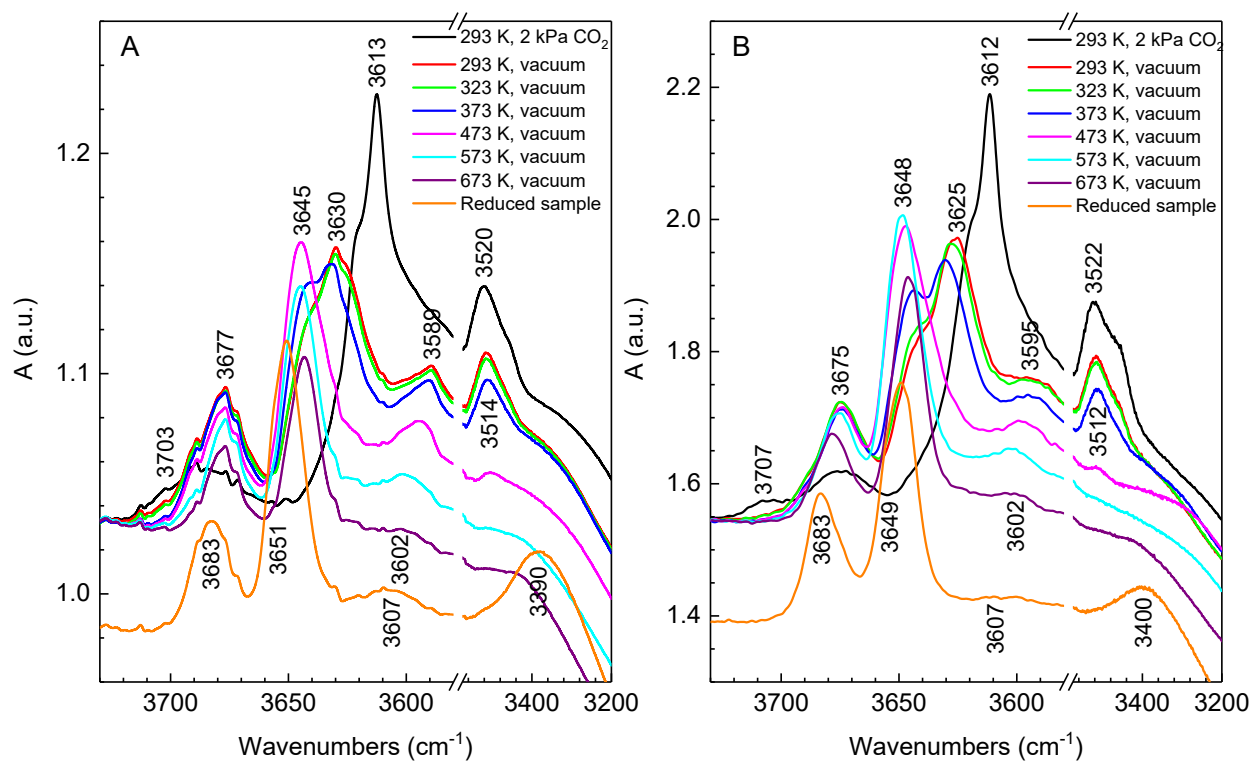
Figure S17. FTIR spectra in the OH-region of H_2-reduced samples obtained after adsorption of 2 kPa (equilibrium pressure) CO_2 at 293 K (black) and evacuation for 10 min at 293 K and elevated temperatures: (A) CeO_2-USRN; (B) CeO_2-AA. See the corresponding spectra in Figs. 8A and S15A.
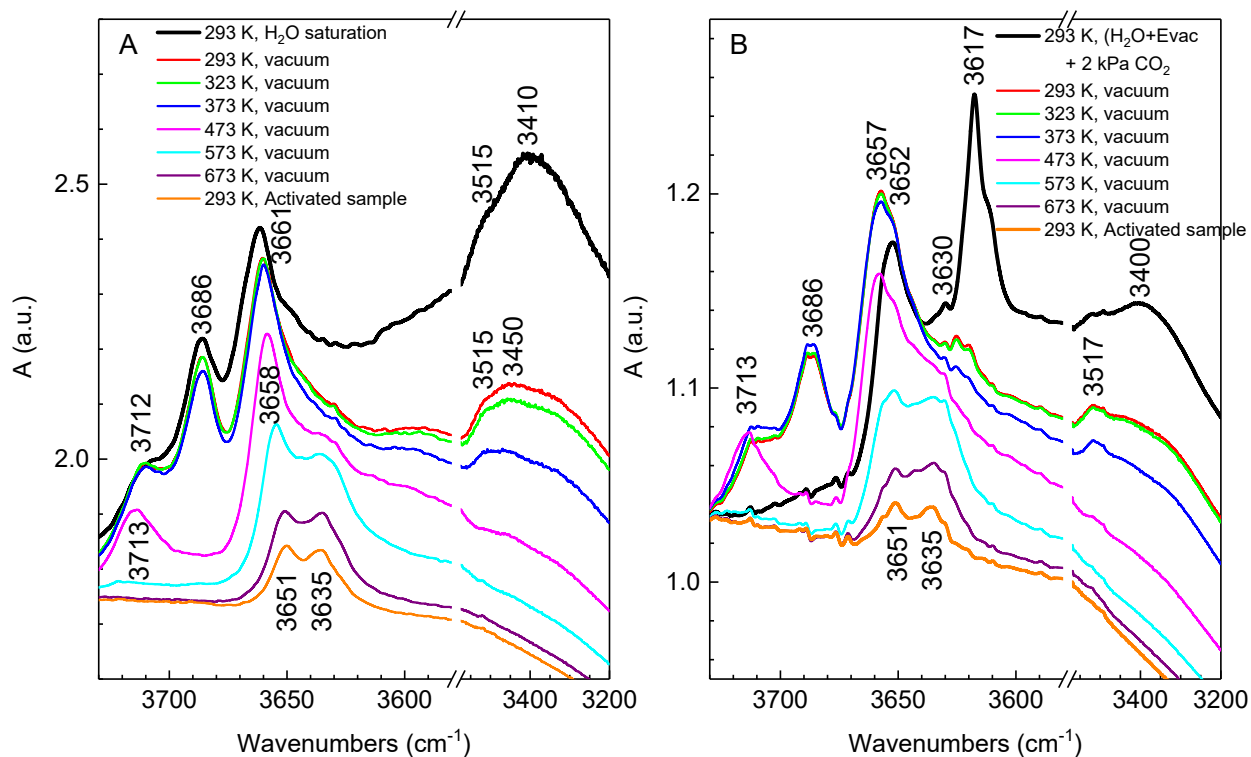
Figure S18. FTIR spectra in the OH-region of the O_2-activated sample CeO_2-USRN obtained after: (A) saturation with H_2O (black, bold) and after evacuation for 10 min at 293 K and elevated temperatures (red to purple, as noted); (B) adsorption of 0.2 kPa H_2O, evacuation at 293 K and adsorption of 2 kPa (equilibrium pressure) CO_2 at 293 K (black, bold); after evacuation for 10 min at 293 K and elevated temperatures (red to purple, as noted), see the corresponding spectra in Fig. 9A.
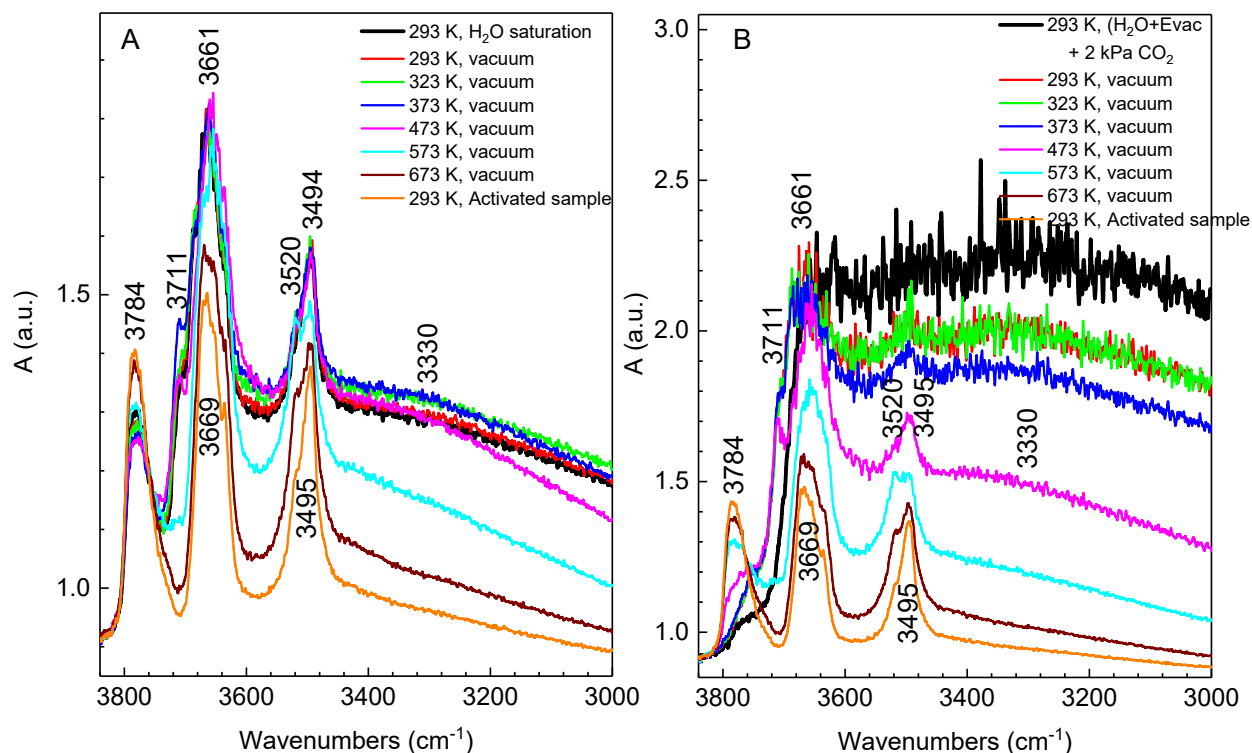
Figure S19. FTIR spectra in the OH-region of the O_2-activated CeO_2-ZrO_2 sample obtained after: (A) saturation with H_2O (black, bold) and after evacuation for 10 min at 293 K and elevated temperatures (red to purple, as noted); (B) adsorption of 0.2 kPa H_2O, evacuation at 293 K and adsorption of 2 kPa (equilibrium pressure) CO_2 at 293 K (black, bold); after evacuation for 10 min at 293 K and elevated temperatures (red to purple, as noted), see the corresponding spectra in Fig. 9B.

1. N. Guillén-Hurtado, I. Atribak, A. Bueno-López and A. García-García, *J. Mol. Catal. A: Chem.*, 2010, **323**, 52-58.
2. F. Zhang, P. Wang, J. Koberstein, S. Khalid and S.-W. Chan, *Surf. Sci.*, 2004, **563**, 74-82.
3. C. M. Sims, R. A. Maier, A. C. Johnston-Peck, J. M. Gorham, V. A. Hackley and B. C. Nelson, *Nanotechnology*, 2019, **30**, 085703-085703.
4. M. V. Rama Rao and T. Shripathi, *J. Electron Spectrosc. Relat. Phenom.*, 1997, **87**, 121-126.
5. A. Laachir, V. Perrichon, A. Badri, J. Lamotte, E. Catherine, J. C. Lavalley, J. El Fallah, L. Hilaire, F. Le Normand, E. Quéméré, G. N. Sauvion and O. Touret, *J. Chem. Soc., Faraday Trans.*, 1991, **87**, 1601-1609.